7896518

Request # 7896518
Ariel To: 134.197.83.20

AUG 22, 2002

Filled

082602

UNIVERSITY OF NEVADA SCHOOL OF MEDICINE
SAVITT DOCUMENT DELIVERY SERVICES/306
1664 NO VIRGINIA ST
RENO, NV 89557-0046

DOCLINE: Journal Copy

Title:	Auditory neuroscience.
Citation:	1996;2(3):219-233
Article:	a model with excitation and inhibition for cells..
Author:	Brughera, AR, Stutman ER
NLM Unique ID:	9607840 ISSN: 1023-618X
Collation:	Serial: Printed language material
Publisher:	Harwood Academic ; Distributed by International Publishers D, [The Netherlands?] : Base
Verify:	Unique Key
Copyright:	Copyright Compliance Guidelines
Authorization:	nmh
Need By:	N/A
Maximum Cost:	**$50.00**
Patron Name:	Macero, Juan Carlos
Referral Reason:	Not owned (title)
Library Groups:	RESOURCE
Phone:	1.775.784-4625x2040
Fax:	1.775.784-4489
Email:	norman@unr.edu
Routing Reason:	Routed to OHUNOU as Refer to Resource Libraries
Received:	Aug 26, 2002 (07:33 AM EST)
Lender:	NEOUCOM (OHIOLINK #211)/ Rootstown/ OH USA (OHUNOU)

Bill to: NVUNEV

UNIVERSITY OF NEVADA SCHOOL OF MEDICINE
SAVITT DOCUMENT DELIVERY SERVICES/306
1664 NO VIRGINIA ST
RENO, NV 89557-0046

Auditory Neuroscience, 1996, Vol 2, pp. 219-233
Reprints available directly from the publisher
Photocopying permitted by license only

A Model with Excitation and Inhibition for Cells in the Medial Superior Olive

ANDREW R. BRUGHERA, ERIC R. STUTMAN, LAUREL H. CARNEY and H. STEVEN COLBURN

Department of Biomedical Engineering, Boston University 44 Cummington Street, Boston, MA 02215

(Received September 19, 1995; Accepted January 12, 1996)

A model that simulates neural discharge patterns of cells in the medial superior olive (MSO) is presented. The model incorporates Hodgkin-Huxley-Eccles models (Rothman *et al.*, 1993) for the activity of cochlear nucleus cells that provide inputs to the MSO. Stochastic inputs to the cochlear nucleus cell models are generated by an auditory nerve model (Carney, 1993). The MSO model incorporates bilateral excitatory inputs from cochlear nucleus cells and inhibitory inputs from brainstem nuclei. The model assumes that the conductance changes associated with inhibitory inputs are relatively long-lasting (several ms) compared with the brief conductance changes (tenths of ms) in the excitatory channels. Responses to tonal stimuli are compared with available MSO data, and responses to click stimuli are compared with data from the inferior colliculus (IC). For the tonal stimuli, realistic dependence on the interaural time delay (ITD) of the MSO discharge rate requires the high degree of synchronization in the model spherical bushy cell excitatory inputs (Joris *et al.*, 1994). For click stimuli, the effect of inhibitory inputs is prominent in the ITD dependence of the response patterns in the IC (Carney and Yin, 1989), and the model requires inhibitory inputs to simulate these responses. Of the four types of inhibitory inputs to the model MSO cell that were tested, only the onset-driven inhibitory inputs reproduced the ITD dependence of click responses without suppressing tone responses.

Key words: auditory, binaural, medial superior olive, neural modeling, computational modeling

Address for Correspondence: Laurel H. Carney, Boston University, Department of Biomedical Engineering, 44 Cummington Street, Boston, MA 02215

THE MEDIAL SUPERIOR OLIVE NUCLEUS (MSO) is one of the first sites in the brainstem where strong binaural interactions take place. MSO cells have long been known to be exquisitely sensitive to changes in the interaural time delay (ITD) of binaural stimuli (Goldberg and Brown, 1969; Yin and Chan, 1990), and are presumed to play an important role in the processing of low-frequency binaural sounds. Binaural processing of complex sounds facilitates not only localization of sounds in space, but also several other phenomena, such as binaural release from masking (Licklider, 1948; review by Durlach and Colburn, 1978), and suppression of reverberations and echoes (Haas, 1951; Gardner, 1968; review by Zurek, 1987). These latter phenomena have received increasing interest from physiologists and modelers in recent years as they provide new ways to relate the physiological response properties of auditory neurons to psychoacoustical performance (Yin and Litovsky, 1993; Yin, 1994).

Models for MSO cells have been useful in contributing to an understanding of the constraints on the neural mechanisms involved in their binaural responses. MSO cells have been described as "EE" cells; that is, they are excited by stimulation of either ear (Goldberg and Brown, 1968). The interactions between the inputs have been most successfully described by a coincidence detection mechanism, which is a special form of running cross-correlation (Yin *et al.*, 1987; Yin and Chan, 1990). Coincidence detection is a relatively simple neural mechanism; a cell simply requires more than one of its inputs to discharge in temporal proximity in order to bring it to threshold. Variations on the number of input discharges required, as well as the temporal window within which the inputs must discharge in order to cause the coincidence-detecting neuron to discharge, are the parameters that shape the response properties of the model cells (Colburn *et al.*, 1990; Carney, 1992; Han and Colburn, 1993). Sensitivity to ITD in model coincidence-detecting neurons depends on the temporal discharge patterns of the inputs from each ear.

Models that have been successful in simulating the ITD sensitivity of MSO neurons to date have not been concerned with the physiological appropriateness of

the models' ion-channel dynamics. In particular, either an instantaneous reset to resting potential upon reaching discharge threshold (Colburn *et al.*, 1990), or very fast potassium channels to repolarize the cells following a discharge (Han and Colburn, 1993) have been assumed. In this study we explored a model for a physiologically realistic coincidence-detecting cell for its ability to simulate the ITD sensitivity of MSO neurons. The model takes advantage of the nonlinear membrane properties that have been described for MSO cells (Smith, 1995). These properties are simulated by a model that was originally developed for cells with similar nonlinear membrane properties in the anteroventral cochlear nucleus (AVCN) (Rothman *et al.*, 1993). This type of model has been shown to be particularly sensitive to the relative timing of its inputs due to the contribution of a slow, low-threshold potassium channel (Stutman, 1993). The model presented here simulates physiological mechanisms that produce both coincidence-detection in bushy cells and MSO cells and high-synchronization inputs to the MSO.

In addition to exploring a physiologically realistic EE model for MSO cells, we studied the potential role of inhibitory inputs to these cells. Inhibitory terminals on MSO cells have been described anatomically (Adams and Mugnaini, 1990; Cant and Hyson, 1992), and inhibitory post-synaptic potentials have been observed in recordings from *in vitro* slice preparations of the MSO (Grothe and Sanes, 1993; Smith, 1995). Inhibitory interactions have also been demonstrated in binaural responses to clicks at the level of the IC (Carney and Yin, 1989). The role of inhibition in binaural processing is not well understood, but may be particularly important for complex phenomena such as the precedence effect, in which the suppression of responses to reverberations and echoes suggests the role of inhibitory effects along the auditory pathway.

Although there are very limited reports on binaural responses to clicks recorded in the MSO *in vivo* (Rupert *et al.*, 1966), there exist related physiological data that make simulations of these responses of interest. Binaural responses to tones from MSO cells are well documented (Goldberg and Brown, 1969; Yin and Chan, 1990), as are binaural responses in the IC to both tones (Rose *et al.*, 1965; Yin and Kuwada, 1983) and clicks (Carney and Yin, 1989). The literature shows that tone responses from principal MSO cells and neurons of the central nucleus of the IC are similar. Therefore similar questions apply to both nuclei concerning the interaction between binaural excitatory and inhibitory mechanisms required to produce the robust tone responses observed in the MSO and IC, and the click responses observed in the IC. We explored the potential effects of several types of inhibitory inputs on both the tone and click responses of the model MSO cell, and examined the ability of the model to replicate both the tone responses in the MSO and click responses from the IC.

METHODS

Description of the Model

The model presented here is for a single principal MSO cell, and incorporates explicit models for selected neurons in the afferent pathways to the MSO. Figure 1 is a schematic diagram of the model and shows the excitatory and inhibitory inputs to the model MSO cell. Model auditory-nerve fibers (AN) (Carney, 1993) act as inputs to bushy cells (BC), and each model bushy cell acts as either an excitatory or inhibitory input to the model MSO cell. For simplicity, the inhibitory interneurons in the trapezoid body, which derive inputs from globular bushy cells and project to the MSO (Cant and Hyson, 1992), have been omitted from the model. The bushy cells and the MSO cell were modeled using a single-compartment Hodgkin-Huxley-Eccles model (Hodgkin and Huxley, 1952; Eccles, 1964) that was previously developed for bushy cells by Rothman *et al.* (1993). The Rothman *et al.* model incorporates a nonlinear membrane conductance common to both bushy cells in the AVCN (Manis and Marx, 1991) and principal cells of the MSO (Smith, 1995). A fourth-order Runge-Kutta-Fehlberg algorithm with a variable step size (Press *et al.*, 1986) was used to solve the differential equations contained in the Hodgkin-Huxley-Eccles point-neuron models.

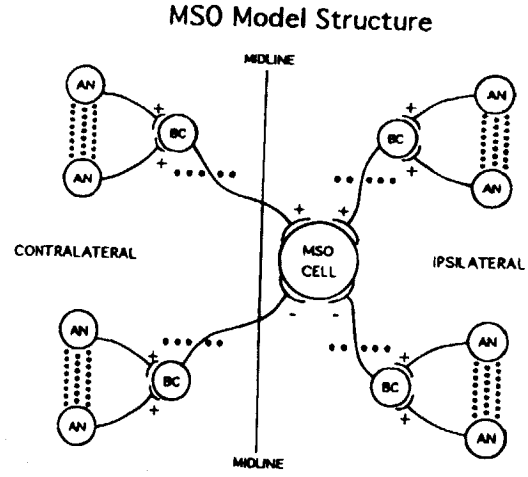

FIGURE 1 **Schematic diagram of the model for an MSO cell.** The diagram illustrates the excitatory and inhibitory input pathways to the model MSO cell. Excitatory synapses are labeled with a '+', and inhibitory synapses with a '–'. The model incorporates explicit models for auditory-nerve fibers (AN) and cochlear nucleus bushy cells (BC). The model MSO cell has 6 excitatory and 6 inhibitory inputs from the ipsilateral side, and an equal number of excitatory and inhibitory inputs from the contralateral side. Each BC receives 20 or 25 AN inputs. Multiple input fibers are denoted with dots. Note that the inhibitory inputs to MSO cells are mediated by trapezoid body neurons that are not explicitly included in the model.

Two exceptions to the form of the model described above were investigated: excitatory inputs to the model MSO cell directly from AN fibers, and separately, level-independent onset-driven inhibitory inputs that were derived without the use of an explicit bushy cell model. Details on the level-independent onset-driven inhibitory inputs are given below in the subsection on the model MSO cell.

Support for our assumption that inhibitory inputs to the MSO can be modeled using bilateral inhibitory inputs relayed from globular bushy cells can be found in the results of anatomical studies. Inhibitory inputs to the MSO are derived from neurons in the trapezoid body that are driven by globular bushy cells. Contralateral globular bushy cells project to the ipsilateral medial nucleus of the trapezoid body (MNTB). Each projection terminates on a principle neuron of the MNTB via a very large and secure synapse, known as a Calyx of Held (Held, 1893; Ramon y Cajal, 1909; review by Irvine, 1986). The principal neurons of the MNTB then project inhibitory inputs ipsilaterally to the MSO (Adams and Mugnaini, 1990; Cant and Hyson, 1992; Smith, 1995). The secure nature of the synapse between globular bushy cell axon and principal MNTB neuron suggests that the discharge patterns of the MNTB neuron would tend to preserve those of the globular bushy cell, and that contralateral inhibitory inputs to the MSO reflect the discharge patterns of contralateral globular bushy cells. In this study, we have assumed that the contralateral inhibitory inputs to the MSO can be modeled as inhibitory inputs relayed from contralateral globular bushy cells. Anatomical evidence also suggests that there is a strictly ipsilateral inhibitory pathway to the MSO. Ipsilateral globular bushy cells drive inhibitory interneurons in the lateral nucleus of the trapezoid body (LNTB) (Smith *et al.*, 1991), and the LNTB projects inhibitory inputs ipsilaterally to the MSO (Cant and Hyson, 1992). A recent physiological study also documents that ipsilateral stimulation of the LNTB in brain-slice preparations elicits an IPSP in the MSO (Smith, 1995). Although calyceal synaptic connections do not appear in the LNTB, one or more ipsilateral projections from globular bushy cells may form large terminals on cell bodies in the LNTB (Smith *et al.*, 1991). In this study, we have assumed that these large synaptic terminals tend to preserve the discharge patterns of their inputs, and that ipsilateral inhibitory inputs to the MSO can be modeled as inhibitory inputs relayed from ipsilateral globular bushy cells.

Model Auditory-nerve Fibers

Discharge patterns of auditory-nerve fibers in response to tones and clicks were simulated using the Carney (1993) model for low-frequency auditory-nerve fibers. This model is characterized by a nonlinear bandpass filter with a time-varying bandwidth that depends upon the level of the input signal. The nonlinear filter is followed by models for discharge generation, including adaptation and absolute and relative refractoriness (Carney, 1993) which contribute to a rate function that drives a non-homogeneous Poisson process.

Refractoriness and adaptation in the Carney model were slightly modified to more closely match those in the Rothman *et al.* (1993) study. Relative refractoriness for the model used in this study was incorporated into the rate function $R(t)$ as follows:

$$R(t) = S(t)[1 - (c_0 e^{-(t-t_l-R_A)/s_0} + c_1 e^{-(t-t_l-R_A)/s_1})]$$
$$for\ (t - t_l) \geq R_A,$$

where $S(t)$ is the probability of discharge before it is affected by refractoriness, t_l is the time of the most recent discharge, and R_A is the absolute refractory period of 0.75 ms ($R(t) = 0$ for $t - t_l < R_A$). The 0.75 ms value for absolute refractoriness was chosen based on previously published modelling work (Carney, 1993). The value of R_A is also comparable to that used in a related modelling study (0.7 ms was used by Rothman *et al.*, 1993). Parameters c_0 (0.55) and c_1 (0.45) are scalars for the two terms describing discharge history effects. Parameters s_0 (0.8 ms) and s_1 (25 ms) are the two time constants describing the discharge history that determines refractoriness (Carney, 1993). In the synapse portion of the Carney model, the maximum values for immediate, local, and global permeabilities PI_{max}, PL_{max}, and PG_{max} were increased to 3.0, 0.2, and 0.1, respectively; these changes were introduced in a preliminary study (Stutman, 1993) and have only minor effects on the shape of the PST histograms at stimulus onset. These parameters determine adaptation in a three-compartment diffusion model. All other parameter values are provided in Carney (1993).

Model Bushy Cells

The Rothman *et al.* (1993) model for bushy cells is described below. The principle equation that describes the soma membrane potential V in the Rothman *et al.* (1993) model is

$$C_S \frac{dV}{dt} + G_B(V - E_K) + G_K(V - E_K) + G_{Na}(V - E_{Na})$$
$$+ G_L(V - E_L) + G_I(V - E_I) + G_E(V - E_E) = I_{ext}$$

where C_S is the membrane capacitance, G_L is the leakage conductance, and I_{ext} is applied external current which is always zero for the simulations described here. C_S and G_L are fixed parameters, as are the reversal potentials for potassium (E_K), sodium (E_{Na}), excitatory inputs (E_E), inhibitory inputs (E_I), and leakage (E_L). G_B, G_K, and G_{Na} are the voltage-and-time sensitive conductances representing the slow potassium, fast potassium, and fast sodium ion-channels. The values of these three con-

ductances are represented in terms of activation variables w, n, and m, and an inactivation variable h, i.e.

$$G_B = G_{B_{max}} w, \quad G_K = G_{K_{max}} n,$$
$$and \quad G_{Na} = G_{Na_{max}} m^2 h.$$

The voltage and time dependencies of the activation and inactivation variables are modeled with Hodgkin-Huxley (1952) type equations of the form

$$\frac{du}{dt} = \alpha_u(1-u) - \beta_u u,$$

where α_u and β_u are rate constants that are dependent on temperature and voltage, and u refers to w, n, m, or h. Rate constants in this study are identical to those used by Rothman *et al.*, which are scaled by a temperature factor (Frankhauser and Moore, 1963) to correct for the difference between mammalian body temperature (38°C) and the temperature at which the data were taken (22°C).

The nonlinear membrane conductance that provides bushy cells with increased sensitivity to the relative times of their inputs is due to the slow, low-threshold potassium channel (Manis and Marx, 1991) described by G_B. These properties are incorporated into three different bushy cell models: Hi-Sync, Pri-notch, and Onset model cells. In each of the bushy cell models, an alpha function with a time constant of 0.1 ms described the timecourse of the excitatory synaptic conductance in response to a single input discharge (Rothman *et al.*, 1993). Mathematically, these changes in conductance are of the form

$$G_E(t-t_n) = G_{E_{max}} \frac{(t-t_n)}{\tau_{ex}} \exp\left[1 - \frac{(t-t_n)}{\tau_{ex}}\right].$$

The changes in conductance begin at the time of the input firing, t_n, have a time constant τ_{ex}, and reach a maximum value of $G_E max$ at time t equal to $(t_n + \tau_{ex})$. No inhibitory inputs were used in the bushy cell models. Input parameters that determine the response types of the model bushy cells are given in Table 1. Further details concerning supporting equations and parameter values in the Rothman *et al.* model can be found in Rothman *et al.* (1993).

The numbers of inputs for the model bushy cells and the MSO cells were chosen primarily on the basis of function (e.g., the ability to simulate physiologically realistic Hi-Sync responses) as opposed to anatomy. With the exception of the large spherical bushy cells, which receive a small number of Endbulb of Held inputs, there is unfortunately little available information in the literature concerning the number of inputs to bushy cells. Liberman (1991) describes the numbers of inputs to bushy cells ranging as high as 50 AN fibers.

Hi-Sync responses result when many slightly subthreshold excitatory inputs with the same CF are input to a model cell (Joris *et al.*, 1994). Synchronization index (SI) (Johnson, 1980) greater than 0.9 and almost perfect entrainment (responses to nearly every cycle of the stimulating tone) are defining characteristics of the Hi-Sync response. These responses have been identified as a spherical bushy cell response type (Smith *et al.*, 1993; Joris *et al.*, 1994), and were used in this study as excitatory inputs to the model MSO cell. Model Hi-Sync cells were also used as inhibitory inputs to the MSO to explore the possible role of Hi-Sync globular bushy cells (Smith *et al.*, 1991; Joris *et al.*, 1994) that may provide inhibition to the MSO via the MNTB and LNTB. Our model Hi-Sync cell had 25 AN inputs with CFs of 500 Hz and peak excitatory conductances of 7 nS. In the Rothman-type point-neuron models used throughout this study, the threshold peak conductance that produced a discharge from a single input firing was approximately 12 nS.

Pri-notch responses and Onset responses were produced by varying the peak conductance and numbers of AN inputs to the model bushy cell. Pri-notch responses were produced with model cells that had 20 AN inputs of weaker strength (peak conductance 3 nS) with a range of CFs from 300–680 Hz, linearly spaced in frequency. Onset responses were produced with model cells that had 20 AN inputs of still weaker strength (peak conductance 1.5 nS) with a range of CFs from 300–680 Hz, linearly spaced in frequency.

Model MSO Cell

The Hodgkin-Huxley-Eccles point neuron model for bushy cells (Rothman *et al.*, 1993) with the slow, low-threshold potassium conductance was also used to

TABLE 1
Input Parameters of Bushy Cell Models

Input Parameter	Type of Model Bushy Cell		
	Hi-Sync	Pri-notch	Onset
number of AN inputs	25	20	20
peak conductance per input	7 nS	3 nS	1.5 nS
range of CFs	500 Hz only	300–680 Hz	300–680 Hz

model the MSO cell. Although membrane properties of MSO cells may differ from those of bushy cells, they are likely to be similar because both types of cells exhibit similar nonlinear membrane resistances (Manis and Marx, 1991; Smith, 1995). The only differences between the Hi-Sync bushy cells and the MSO cells in the model were the type of inputs and the associated conductance parameters. Six types of model MSO cells were explored, and the excitatory and inhibitory inputs used in each type of model MSO cell are as follows:

1. Hi-Sync excitatory inputs only
2. AN excitatory inputs only (tone responses only)
3. Hi-Sync excitatory inputs, Hi-Sync inhibitory inputs
4. Hi-Sync excitatory inputs, Pri-notch inhibitory inputs
5. Hi-Sync excitatory inputs, Onset inhibitory inputs
6. Hi-Sync excitatory inputs, Level-Independent Onset inhibitory inputs (click responses only; no explicit AN or bushy cell models in the inhibitory pathway)

The input parameters for the six types of model MSO cells are given in Table 2.

All MSO model cells received six excitatory inputs from each side of the brainstem. As in the bushy cell models, an alpha function with time constant τ_{ex} of 0.1 ms described the timecourse of the excitatory synaptic conductance in response to a single input discharge. The amplitudes of the conductances ($G_E max$) were varied to investigate the sensitivity of the model to this parameter, and a value of 2.5 nS was chosen for the bushy cell inputs to the MSO cell. With this value the discharge rate as a function of ITD in the model was slightly greater than in physiological data for tone responses (Goldberg and Brown, 1969). This was done with the expectation that introducing inhibitory inputs to the model would reduce discharge rates to within the physiologically observed range.

In the simulations involving bilateral inhibition to the model MSO from each of the three bushy cell response types, the model MSO cell received six inhibitory inputs from each side of the brainstem. The time constant (τ_{inh}) of the alpha functions for the inhibitory conductances was set to 4 ms. This value is generally consistent with recent physiological observations (Smith, 1995). The amplitudes of the conductances ($G_I max$) were varied to determine the upper limit for each type of inhibitory input based on the criterion that the discharge rate of the tone response of the model remained within the physiological range.

For the simulations with inhibitory inputs relayed from globular bushy cells, there was no additional delay added to inhibitory inputs; however, the longer time constant of the alpha functions describing inhibitory inputs effectively contributes a delay to the inhibitory pathway. In response to a stimulus from a given side, the difference between inhibitory and excitatory time constants produces a maximum in the inhibitory conductance approximately 3.9 ms after the maximum in excitatory conductance.

In addition to the model MSO cells with inhibitory inputs from bushy cell models, a model MSO cell was investigated in which the six inhibitory inputs from each side of the brainstem were ideal onset cells with level-independent responses. No explicit AN models or bushy cell models were used in the inhibitory pathway, and only click responses were simulated with this model. Click stimuli produced one input firing on each

TABLE 2
Input Parameters of the Six Models of the MSO Cell

Excitatory Inputs:

Model #	Type of Inputs	# Inputs/Side	$G_{E_{max}}$	Basis Function	τ_{ex}
1	Hi-Sync	6	2.5 nS	alpha	0.1 ms
2	AN	6	4.0 nS	alpha	0.1 ms
3	Hi-Sync	6	2.5 nS	alpha	0.1 ms
4	Hi-Sync	6	2.5 nS	alpha	0.1 ms
5	Hi-Sync	6	2.5 nS	alpha	0.1 ms
6	Hi-Sync	6	2.5 nS	alpha	0.1 ms

Inhibitory Inputs:

Model #	Type of Inputs	# Inputs/Side	$G_{I_{max}}$	Basis Function	τ_{inh}
1	n/a	0	n/a	n/a	n/a
2	n/a	0	n/a	n/a	n/a
3	Hi-Sync	6	0.3 nS	alpha	4 ms
4	Pri-notch	6	1.0 nS	alpha	4 ms
5	Onset	6	4.0 nS	alpha	4 ms
6	Level-Ind. Onset	6	10.0 nS	exponential	6 ms

of the inhibitory inputs. The input firings occurred 6 ms after the click at the corresponding ear. The 6-ms delay of the inhibitory inputs was chosen so that the inhibitory response occurred approximately 1 ms after the excitatory response from the model bushy cells, which have a latency period of 5 ms that is due to the latency of the auditory-nerve model. The inhibitory inputs were made identical for clicks over the intensity range from 40 to 80 dB peak-equivalent SPL. The time course of the inhibitory conductances for each input was described by a step increment to 10 nS followed by an exponential decay with a time constant of 6 ms. Thus the step-increment inhibitory conductance in these simulations reached its maximum approximately 1 ms after the maximum in excitatory conductance.

Stimuli

The acoustic waveform for each stimulus type and level was used as the input to the Carney model. Simulated discharge times were generated for 270 independent auditory-nerve fibers for each ear. The times of neural discharge from 25 (or 20, for some bushy cell models) auditory-nerve fibers were used as inputs to each model bushy cell. The times of discharge from the model bushy cells were generated and used as inputs to the model MSO cell. Neither synaptic delays nor transmission delays were included in the model, so that the onset delays are dominated by the latency of the responses of the AN model. No internal interaural delays were imposed; therefore the characteristic delay of every model MSO cell is fixed at zero. The ITD of the stimulus was introduced in the model by adding a delay to the discharge times of inputs to the MSO from one side of the brainstem. For both tonal and click inputs, 0.2-ms increments in ITD were used throughout the simulations.

Low frequency tones of 500 Hz at 70 dB SPL with a duration of 500 ms, presented at time intervals of 800 ms, were used to evaluate the steady-state properties of the MSO model. Binaural click stimuli in the form of 100-μs pulses were used to evaluate the transient response of the model MSO cell. Successive binaural clicks were separated by time intervals of 100 ms. Click intensity was quantified in terms of peak-equivalent SPL, i.e., the click amplitude was specified as the rms pressure in dB SPL of a tone that had a peak amplitude equal to that of the click.

Analysis Procedures

Analyses of simulations were chosen to replicate those used in physiological studies. In simulations using tonal stimuli, the times of discharge by the model MSO cell were recorded during binaural stimuli at selected values of ITD, and during monaural stimuli. Discharge rate and SI were calculated and plotted as functions of ITD. In simulations using click stimuli, rate-ITD functions (in this case, the number of spikes per stimulus as a function of ITD) and dot raster displays were generated. The dot rasters were generated using times of discharge from the model MSO cell for values of ITD from −30 to 30 ms at 1-ms intervals.

RESULTS

Model Bushy Cells

Figure 2 shows PSTHs of Hi-Sync, Pri-notch, and Onset type bushy cell models in response to 200 repetitions of a 25-ms, 500-Hz tone-burst at 70 dB SPL. The response of the model Hi-Sync cell (Fig. 2A) to the tone-burst is characterized by a high degree of phase-locking (SI = 0.9), and a high discharge rate during both the onset response and steady-state response. The high degree of phase-locking is illustrated in the histogram by the presence of sharp peaks separated by the period of the stimulus, with very few discharges between peaks. After a latency period of 5 ms, the model cell discharged within the first peak of the PSTH in 198 of 200 of stimulus repetitions. During the steady-state portion of the response (from 10–25 ms after onset of the tone), the discharge rate was 497 spikes/sec, with an entrainment index (Joris *et al.*, 1994) equal to 0.98.

The model Pri-notch cell's response (Fig. 2B) is characterized by a robust onset response, and a significantly weaker steady-state response than for the Hi-Sync model cell. The model Pri-notch cell discharged strongly at the onset of the tone with responses in the first peak on 198 of the 200 stimulus repetitions, and the steady-state discharge rate was 140 spikes/sec.

The model Onset cell's response (Fig. 2C) has a moderately strong onset response, and almost no steady-state response. This cell responded during the first peak in 139 of the 200 stimulus repetitions. The model Onset cell was effective in providing onset-driven inhibition for tones and clicks at 60 dB peak-equivalent SPL or higher. At 60 dB or higher the strength of the onset response of the model Onset cell was comparable the that of the model Hi-Sync cell. However, below 60 dB SPL the model Onset cell produced very infrequent discharges even at onset in comparison to the model Hi-Sync cell. Although increasing the excitatory conductance amplitude increased the onset response, it also increased the steady-state response of the model Onset cell. An attempt was made to increase the onset response without increasing steady-state response by increasing the synaptic strength and increasing the range of CFs to 100–860 Hz. However, the onset response could not be increased without increasing the steady-state response.

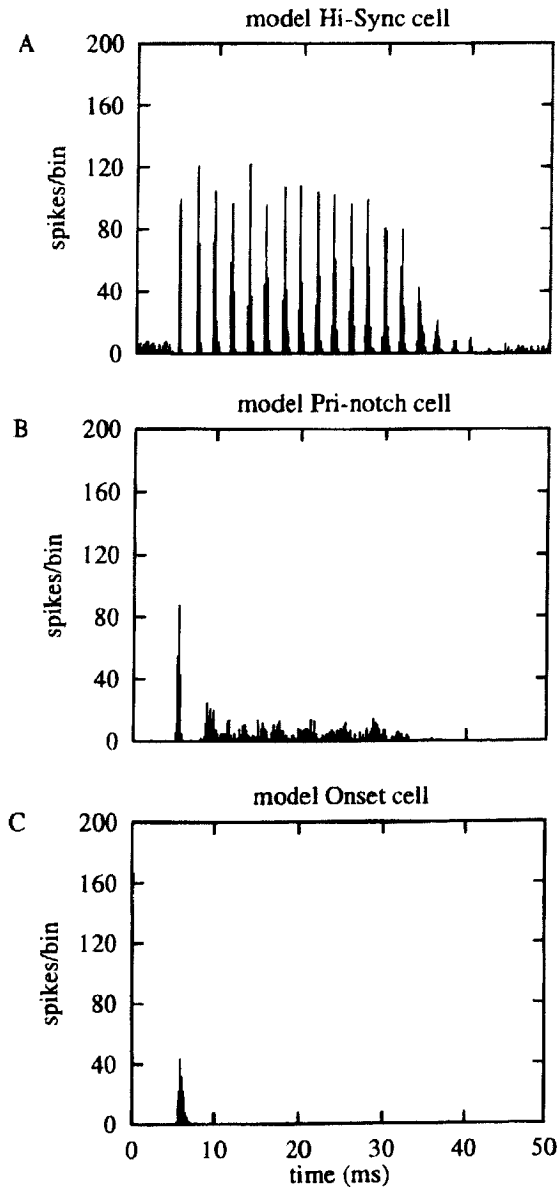

FIGURE 2 **PST histograms from bushy cell models.** The figure illustrates responses from three types of model bushy cells that act as inputs to the model MSO cell. (A) Hi-Sync model bushy cell, (B) Pri-notch model bushy cell, (C) Onset model bushy cell. Stimuli were 200 repetitions of a 25-ms, 500-Hz tone-burst at 70 dB SPL. Histogram binwidth was 0.2 ms.

Model MSO Cell—Role of Hi-Sync Excitatory Inputs

In Fig. 3, the ability of the model MSO cell to achieve highly modulated rate-ITD curves and a high synchronization index (SI) are compared for AN excitatory inputs (SI = 0.7) and Hi-Sync bushy cell excitatory inputs (SI = 0.9). Under stimulation with a 500-Hz tone at 70 dB SPL, the response of an MSO model cell that received 12 model AN inputs was compared with the response of a model cell that received 12 Hi-Sync inputs in its ability to match responses from an MSO cell to a 434-Hz tone (Goldberg and Brown, 1969).

The empirical rate-ITD curves (Fig. 3A) and SI-ITD curves (Fig. 3B) are well described by the model MSO cell with 12 Hi-Sync inputs (Figs. 3C and 3D). Also similar to data from MSO cells (Yin and Chan, 1990), the model with Hi-Sync inputs produced discharge rates at the minima of the rate-ITD curves that were lower than the monaural discharge rate.

The empirical data are not well characterized by the model cell with 12 AN inputs (Figs. 3E and 3F). In this model, the peak-to-peak amplitude of modulation in the rate-ITD was less than that observed in the physiological data, and maximum values of SI were below those in the data. In addition, the discharge rate at the minima of the rate-ITD curves is higher than the monaural discharge rate, which is uncharacteristic of MSO cells (Yin and Chan, 1990). The number of AN inputs was increased to a maximum of 40. With this number of inputs the rate-ITD curve matched the data, but the maximum SI remained less than 0.8. Monaural stimuli were not applied to the model MSO with 40 AN inputs.

Model MSO Cell—Excitatory and Inhibitory Responses to Tones

In this subsection we described the results of adding each of the three bushy cell response types as inhibitory inputs relayed to the model MSO cell. In each case, the excitatory inputs were 6 Hi-Sync inputs with conductance amplitudes of 2.5 nS from each side of the brainstem (see Fig. 1).

Rate-ITD curves are shown for each type of inhibitory input for increasing values of peak inhibitory conductance in Fig. 4. Each type of inhibitory input suppressed to a different degree the tone response of the model MSO cell. With Hi-Sync inhibitory inputs (Fig. 4A), rate-ITD curves were strongly suppressed due to the high steady-state discharge rates of these inputs. With Pri-notch inhibitory inputs (Fig. 4B), rate-ITD curves showed weaker suppression of the ITD curve due to the weak sustained rate of the model Pri-notch cell. Onset inhibitory inputs (Fig. 4C) had very little effect on the rate-ITD curves for sustained tones, even for very large values of inhibitory conductance.

For Hi-Sync and Pri-notch inhibitory inputs, we determined the highest value of the peak inhibitory conductance per input that would still result in a tone response within the physiologically observed range (Yin and Chan, 1990), and used these values in simulations of click responses. The maximum peak conductance values per inhibitory input values were 0.3 nS for Hi-Sync inhibition, and 1.0 nS for Pri-notch inhibition when the maximum excitatory conductance $G_E max$ was set to 2.5 nS. For Onset inhibition, no real constraint was imposed on the inhibitory conductance

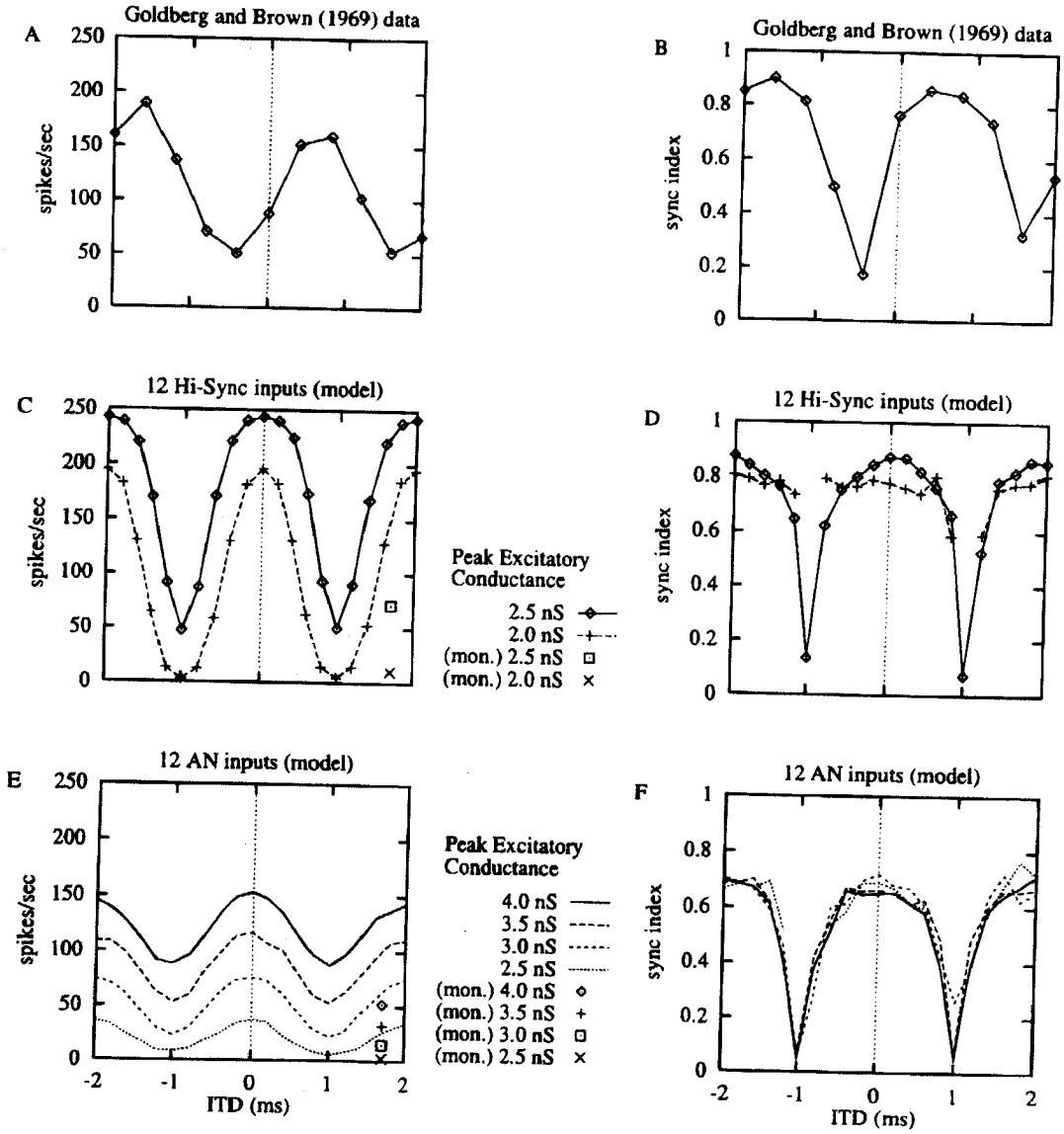

FIGURE 3 **Discharge rate and synchronization index as a function of ITD in MSO cells (responses of Unit 67-82-5 from Goldberg and Brown (1969), with permission) and model MSO cells under stimulation with low-frequency steady-state tones.** (A) rate-ITD curve from MSO cell, (B) sync-ITD curve from MSO cell, (C) rate-ITD curves and monaural discharge rates from model MSO cell with 12 Hi-Sync inputs, (D) sync-ITD curves from model MSO cell with 12 Hi-Sync inputs, (E) rate-ITD curves and monaural discharge rates from model MSO cell with 12 AN inputs, (F) sync-ITD curves from model MSO cell with 12 AN inputs. Effects of varying peak excitatory conductance are shown for the two models. Note the difference in ranges of peak conductance between panels (C,D) and (E,F). Points in the SI-ITD curves meet the Rayleigh Criterion for statistical significance ($P < .01$), with a bimodal distribution assumed for points at minima (Rayleigh, 1919; Mardia, 1972). Hi-sync excitatory inputs with peak conductance of 2.5 nS are maintained throughout model results shown in subsequent figures.

amplitude by the tone response, and the peak inhibitory conductance per input was set to match click responses measured in the IC.

Model MSO Cell—Excitatory Responses to Clicks

Figure 5 shows the two major characteristics in empirical click responses from the IC (Carney and Yin, 1989) that we explored with this model. The first is the modulation in the number of spikes per stimulus as a function of ITD (Fig. 5A). The second is the suppression of the response to the delayed click. In the example shown, this suppression occurs for ITDs less than 10 ms, and releases gradually for larger ITDs. The rate-ITD function (Fig. 5B) shows the reduction in the number of spikes for a range of ITD around zero, and the dot raster (Fig. 5C) shows that the reduction is due to suppression of the response

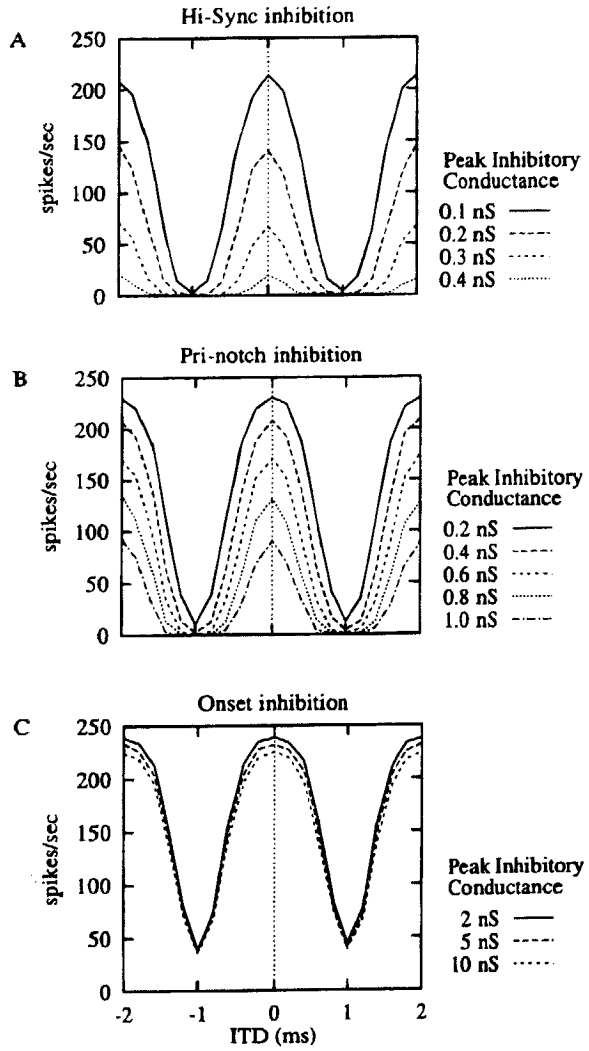

FIGURE 4 **Rate-ITD curves for tones for model MSO cells receiving three different histogram types of inhibitory input: (A) Hi-Sync, (B) Pri-notch, and (C) Onset.** Effects of increasing inhibitory synaptic conductance are shown. Note that the range of conductance amplitude is different in each panel. For Hi-Sync and Pri-notch inhibitory inputs, upper limits on peak inhibitory conductance that resulted in tone-responses within physiological range were determined (0.3 nS for Hi-Sync; 1 nS for Pri-notch). Onset inhibitory inputs have a negligible effect on the steady-state rate-ITD curves. Increments in ITD of 0.2 ms were used in all simulations involving varying ITD.

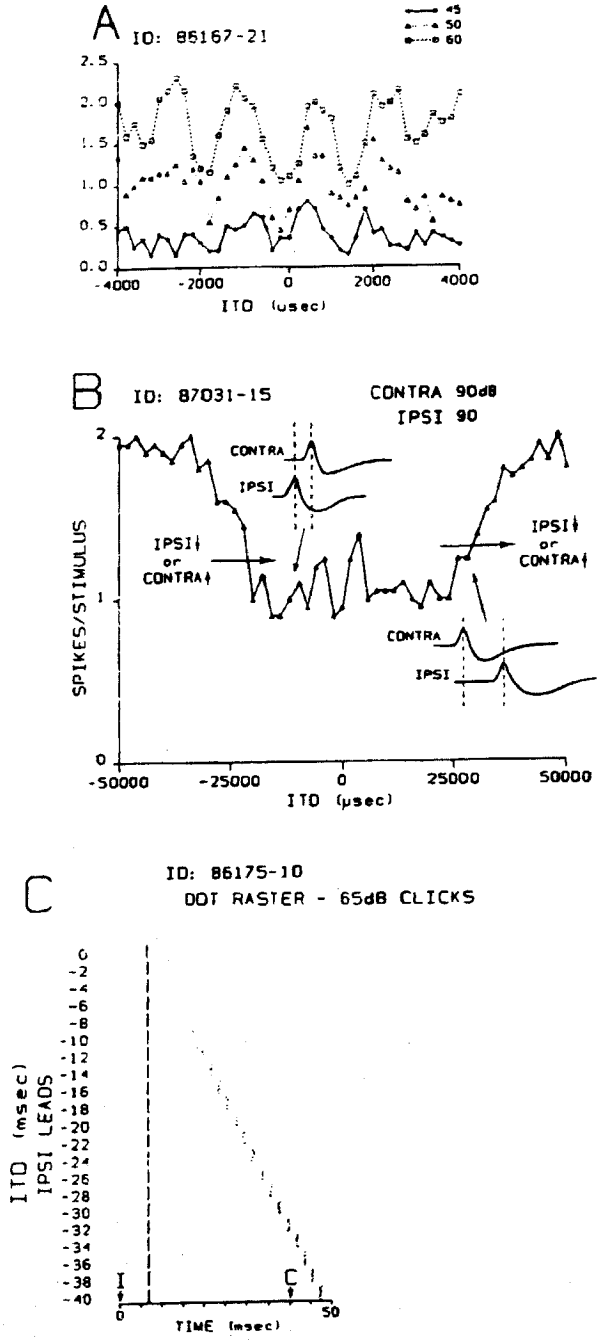

FIGURE 5 **Responses to clicks in the IC (Carney and Yin, 1989) (reprinted with permission).** Data from three different neurons showing characteristics representative of neurons in the IC: (A) modulation with period (1/CF) in the rate-ITD function for small values of ITD (Fig. 4E from Carney and Yin), (B) transition in the rate-ITD function from 1 to 2 spikes/stimulus as ITD is increased (Fig. 8A from Carney and Yin), and (C) inhibitory suppression of the response to the lagging click for values of ITD less than 10 ms (Fig. 5E from Carney and Yin). Release of suppression at large ITD is reflected in the transition in the rate-ITD function.

to the click at the lagging ear. These examples were selected from different neurons to show typical behavior.

Responses to click stimuli are shown in Fig. 6 for the model MSO cell without inhibition (Hi-Sync excitatory inputs only). Rate-ITD curves from the model for click intensities of 40, 60, and 80 dB peak-equivalent SPL show reduced rates at small ITDs and modulation at the CF of the model cell (Fig. 6A). The number

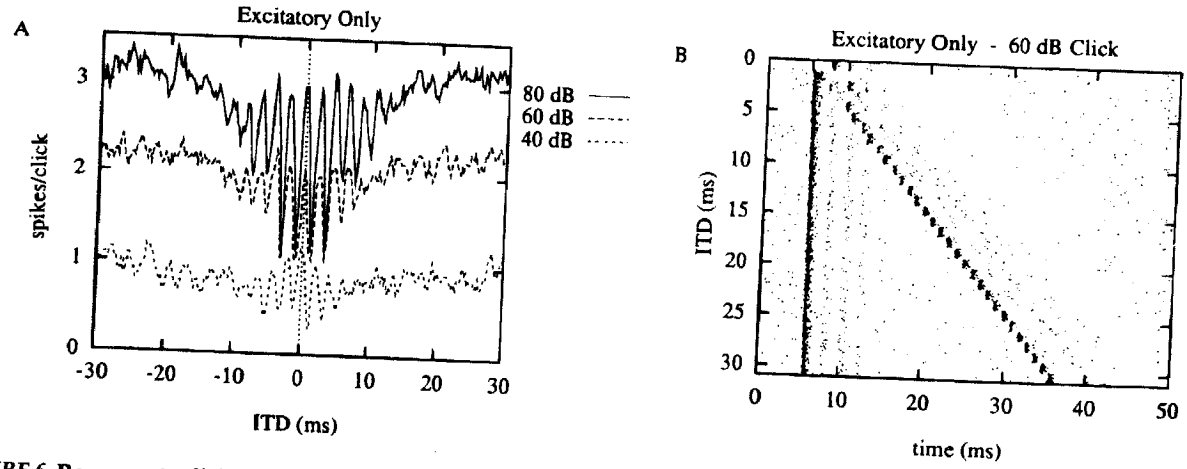

FIGURE 6 **Response to clicks of the model MSO cell with no inhibition (Hi-Sync excitatory inputs only):** (A) rate-ITD functions for clicks at 40, 60, and 80 dB peak-equivalent SPL, and (B) dot raster for the click at 60 dB. The dot raster was prepared using 1-ms increments in ITD.

of discharges per binaural click stimulus (spikes/clk) were counted over a window that began at the time the click was applied to the AN model and had a duration of 15 ms plus the ITD. The modulation in the number of spikes per stimulus is due to the binaural interaction of the inputs from the model Hi-Sync cells, and becomes more pronounced and prolonged at higher intensities. This level dependence is due to an increase with level in the strength and duration of the click responses in the model Hi-Sync cells that act as inputs to the model MSO. The dot raster display (Fig. 6B) shows the temporal pattern of firing for values of ITD from 0 to 30 ms. The negative range was omitted because bilateral symmetry in the model made the dot raster for negative ITDs nearly identical to that for positive ITDs. The effects of refractoriness can be seen in the dot raster by the absence of a response to the second click at ITDs of 1 and 3 ms, and in the band of reduced firings in the temporal region following the response to the second click.

Model MSO Cell—Excitatory and Inhibitory Responses to Clicks

Simulation results are shown in Fig. 7 for model MSO cells with three types of inhibitory inputs: Hi-Sync (Fig. 7A, B), Pri-notch (Fig. 7C,D), and Onset (Fig. 7E,F). As in the models for tone responses and purely excitatory click responses, the model MSO cell received 6 excitatory inputs per side from Hi-Sync bushy cell models with peak conductance of 2.5 nS. Peak inhibitory conductances, $G_i max$, for the Hi-Sync and Pri-notch inhibitory inputs were set to the highest values for which physiologically realistic tone responses were obtained: 0.3 nS for Hi-Sync, and 1 nS for Pri-notch. For the Onset inhibitory inputs, peak inhibitory conductances were set to 4 nS in order to match the ITD sensitivity in the response to clicks from IC cells in previous studies. These simulations of combined excitatory and inhibitory responses to clicks were obtained for click intensities of 40, 60, and 80 dB peak-equivalent SPL, for ITD values between –30 and 30 ms. The rate-ITD functions for all three click intensities are shown, along with a dot-raster display of results for a single intensity. The intensity shown is that at which results were the best approximation to the IC data, i.e., the dot raster which showed the greatest suppression of the response to the click at the lagging ear. The negative range of ITD was omitted from the dot raster because results were nearly identical to those for positive ITDs.

The dot-rasters from simulations with Hi-Sync and Pri-notch inhibitory inputs (Fig. 7B,D) do not show as much onset-driven inhibition as seen in IC click responses. There is not a clear suppression of the response to the click at the lagging ear. Modulation of the rate-ITD curve, which was driven by excitatory activity in the model, remains prominent for the model MSO cell with Hi-Sync and Pri-notch inhibitory inputs (Fig. 7A,C), particularly at higher intensities.

In the simulations with inhibitory inputs from model Onset cells, the dot raster (Fig. 7F) shows a clear suppression of the response to the 80 dB click in the lagging ear. The rate-ITD function for the 60 dB click is consistent with a partial suppression of the response to the click at the lagging ear. Note that the rate-ITD curve for the click at 80 dB is below that at 60 dB because the discharge rate of the click response of the model Onset cell increases sharply between 60 and 80 dB, more sharply than the click response of the excitatory model Hi-Sync input. The degree of modulation in the rate-ITD curves is less for the Onset inhibitory inputs than for the Hi-Sync and Pri-notch inhibitory

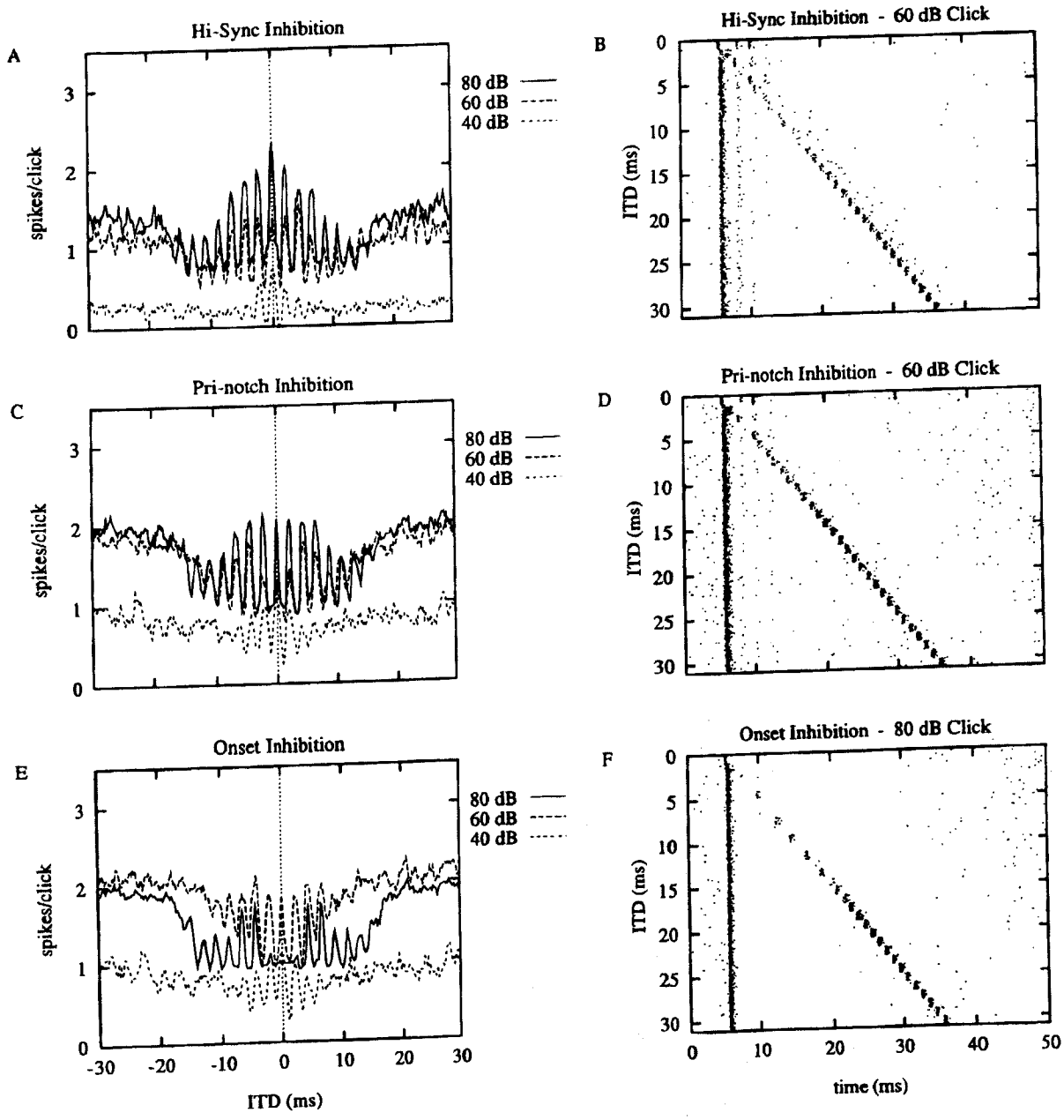

FIGURE 7 **Combined excitatory and inhibitory responses to clicks in the model MSO cell—comparison of response with 3 different types of inhibitory inputs.** Rate-ITD functions at click intensities of 40, 60, and 80 dB peak-equivalent SPL. Dot rasters shown for each type of inhibitory input are at the intensity at which the model shows the greatest suppression of the response to the click at the lagging ear in Figures 5B and 5C. (A) rate-ITD functions for model with Hi-Sync inhibitory inputs, (B) dot raster for model with Hi-Sync inhibitory inputs (click at 60 dB), (C) rate-ITD functions for model with Pri-notch inhibitory inputs, (D) dot raster for model with Hi-Sync inhibitory inputs (click at 60 dB), (E) rate-ITD functions for model with Onset inhibitory inputs, (F) dot raster for model with Onset inhibitory inputs (click at 80 dB). The dot rasters were prepared using 1-ms increments in ITD.

inputs. The Onset inhibition which suppresses the response to the lagging click reduces the amount of modulation in the rate-ITD curve.

Figure 8 shows click responses in the form of rate-ITD curves (Fig. 8A) and dot raster displays (Fig. 8B–E) for a model MSO cell with level-independent, onset-driven inhibitory inputs. Responses were generated for clicks of intensities 40, 50, 60, and 80 dB peak-equivalent SPL. Note that for all intensities tested the response to the lagging click is almost completely suppressed for ITDs of less than 10 ms. For the click at 40 dB, the model responded most strongly to a binaural

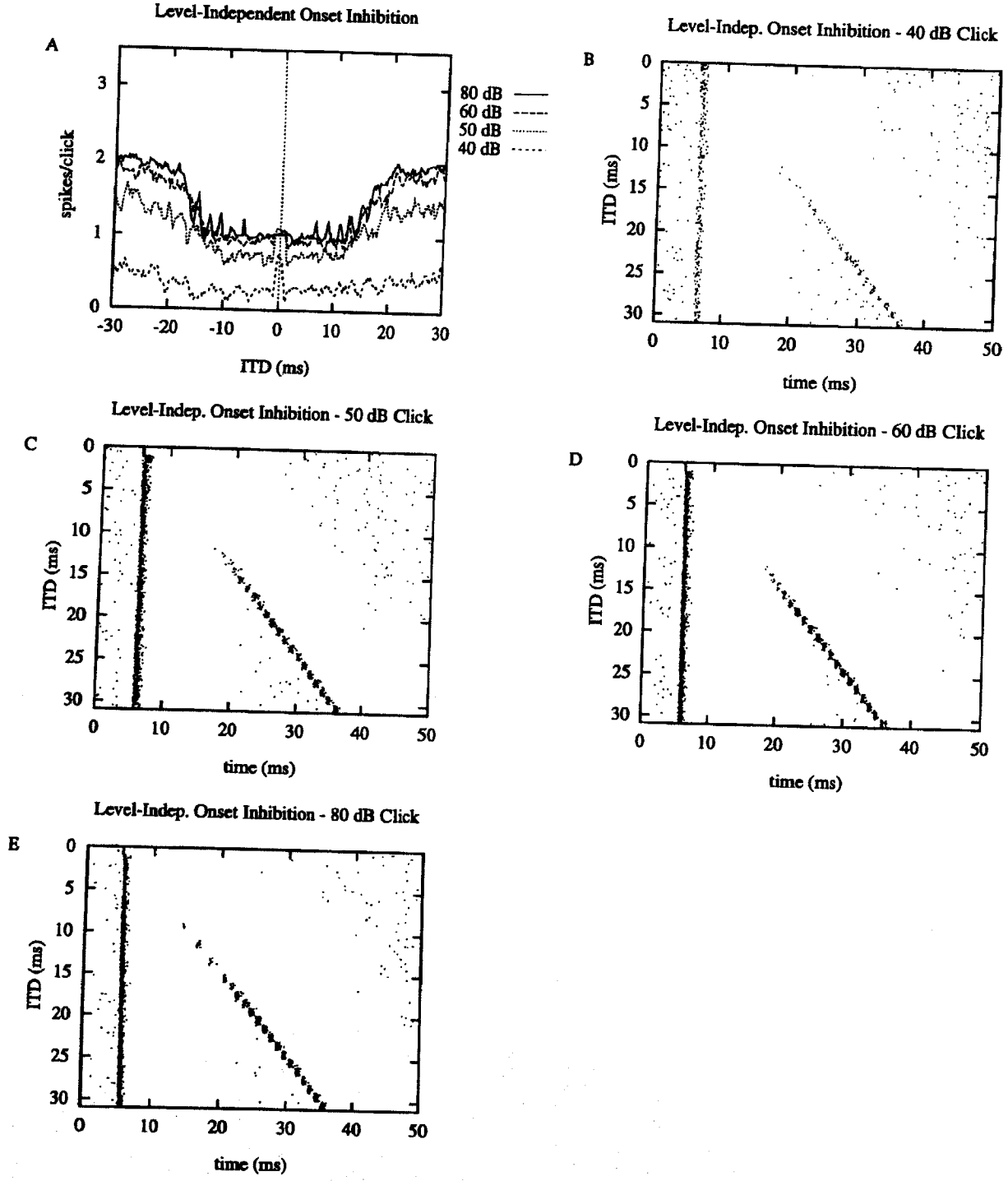

FIGURE 8 **Click responses for the model MSO cell with level-independent Onset inhibition.** (A) Rate-ITD functions for clicks of intensities, 40, 50, 60, and 80 dB peak-equivalent SPL. At 40 dB, the maxima in the function is at the characteristic delay of the cell (ITD = 0 ms). The response at 40 dB is similar to that of IC neurons stimulated with lower intensity; binaural coincidence of inputs is necessary to produce a strong response. The rate-ITD function at 50 dB has a local maxima at an ITD equal to zero, but stronger monaural response at this intensity produces an absolute maxima in the function at a large value of ITD. The response at 50 dB is intermediate between those at 40 and 60 dB. At 60 and 80 dB, 1 spike/click occurs for smaller values of ITD, and 2 spikes/click occur for larger values of ITD, with a transition from 1 to 2 spikes/click occurring for ITD between 10 and 20 ms. (B-E) Dot rasters for click intensities of (B) 40 dB, (C) 50 dB, (D) 60 dB, and (E) 80 dB. For ITD less than 10 ms, suppression of the response to the lagging click is present at all intensities. The dot rasters were prepared using 1-ms increments in ITD.

click with an ITD of zero, the characteristic delay of the cell, although there is a weak response to the leading click for non-zero values of ITD. At 50 dB, there is a local maxima in the rate-ITD curve (Fig. 8A) at an ITD of zero, but the higher intensity causes a stronger response at larger ITDs than produced at 40 dB because the response to both leading and lagging clicks is stronger. At 60 and 80 dB, the model always discharges in response to the leading click (Fig. 8D and 8E) independent of ITD, and responds robustly to the lagging click for ITDs greater than 20 ms. Note that unlike the model with Onset inhibition from the bushy cell model, the rate-ITD functions for this model show a slight increase in the number of spikes/click at 80 dB, compared with 60 dB. For all intensities tested, the inhibition due to the leading click has nearly completely dissipated after 20 ms, and the model responds equally to leading and lagging clicks at these large ITDs. The response to the lagging click recovers slightly more quickly at 80 dB than at lower intensities due to increased excitatory activity at the higher intensity. Note that this early recovery occurs for values of ITD equal to 10, 12, and 14 ms (and not for 11, 13, and 15 ms), indicating that binaural interaction between the excitatory input patterns from both the leading and lagging clicks are necessary to produce these discharges.

DISCUSSION

We have explored six models for principal cells of the MSO: two models for MSO cells with only excitatory inputs, and four models with both excitatory and inhibitory inputs. The purely excitatory model with Hi-Sync inputs was superior to a model with AN inputs in simulating tone responses of MSO cells. The Hi-Sync excitatory inputs from model bushy cells that simulate the activity of cochlear nucleus neurons were subsequently used in the models that included inhibitory inputs. The four models with inhibition differ in the nature of the inhibitory inputs to the model MSO cell. These models include cases with inhibition from Hi-Sync, Onset-with-low-sustained-rate, Onset, and level-independent Onset cells.

Simulation results demonstrate that, given Hi-Sync excitatory inputs, the steady-state tonal responses observed in the MSO (Goldberg and Brown, 1969; Yin and Chan, 1990) can be generated from any of the models considered here. Although the tonal response places constraints on the conductance amplitude of Hi-Sync and Pri-notch inhibitory inputs, it appears that neither the presence of inhibitory inputs nor the response-type of those inputs is constrained by the observed tonal responses. This result is consistent with the modeling studies of Colburn *et al.* (1990) and Han and Colburn (1993), who showed that the observed dependence of firing rate and synchronization on ITD are not dependent on an inhibitory mechanism even though, at unfavorable ITDs, the response to binaural stimulation results in firing rates below the firing rate observed in response to stimulation by the waveform presented to either ear alone. All of these studies are consistent with the conclusion that tonal stimuli are not appropriate for exploring the role of inhibitory inputs to the MSO.

In the current study it appears that observed MSO firing patterns depend primarily on short duration excitatory inputs from Hi-Sync response type cells in the cochlear nucleus. The short-duration post-synaptic potentials are the result of the nonlinear membrane properties introduced by the slow, low-threshold potassium channel in the cell model (Rothman *et al.*, 1993). It also appears that in the steady-state portion of the tonal response, the effective conductance changes due to the excitatory inputs must be relatively large compared with the conductance changes due to inhibitory inputs.

When simulations for click stimuli are compared with data from the IC, several results are notable. First, when the inhibition arises from Hi-Sync inputs, there is a conflict between generating the amount of suppression observed in the IC (Carney and Yin, 1989) and maintaining the rate-ITD curves and synchronization observed in the MSO in response to tones. This difficulty with Hi-Sync inhibitory inputs may be a problem for simple models for firing patterns at any level which show robust responses to tones and significant inhibitory effects in responses to clicks. Second, if inhibitory inputs are provided by neurons of the Onset or Pri-notch type (especially those with low sustained rates, e.g. O_L), it is possible to generate patterns for steady tones that are consistent with observed ITD dependence and patterns for clicks that show the transient suppression as observed in the IC. Third, when the ITD dependence of the responses to clicks are compared for a variety of intensity levels, it becomes clear that the simulations are most representative of the data when the onset inhibitory input patterns are independent of level. Thus the onset-driven inputs underlying the inhibition must have relatively steep rate-level functions that reach high discharge rates at lower levels than did our Onset-type bushy cell model.

There is a problem in postulating the existence of onset-driven inhibition in the MSO because there is no evidence for this type of inhibitory input to the MSO. Recent anatomical and physiological evidence indicates that sources of inhibition to the MSO are more likely to have Hi-Sync responses than Onset responses. Principal neurons in the MNTB which project inhibitory inputs to the MSO are driven by globular bushy cells that, for CFs below 1 kHz, have very high levels of synchronization compared with auditory-nerve fibers (Smith *et al.*, 1991; Joris *et al.*, 1994). Principal neurons of the MNTB are driven via the

large, secure Calyx of Held synapses, with each calyx terminating on a single principal neuron and each principal neuron receiving only one calyx (Held, 1893; Ramon y Cajal, 1909; review by Irvine, 1986). This type of synaptic configuration would tend to preserve the temporal discharge patterns of the globular bushy cell in the discharges of the MNTB neuron, and suggests that the response types of principal MNTB neurons with low CF are also Hi-Sync. Given also the high percentage of Hi-Sync responses among low-CF globular bushy cells (Joris *et al.*, 1994), it seems likely that inhibitory inputs to the MSO are relayed from Hi-Sync globular bushy cells with low CFs, via inhibitory interneurons in the MNTB. These inhibitory inputs to the MSO are from the ipsilateral MNTB via contralateral globular bushy cells (Adams and Mugnaini, 1990; Cant and Hyson, 1992; Smith, 1995). Anatomical evidence also suggests that there exist inhibitory inputs to the MSO driven by ipsilateral globular bushy cells via inhibitory interneurons in the ipsilateral LNTB (Cant and Hyson, 1992; Smith, 1995). Although this evidence does not include a calyceal synaptic connection in the LNTB, the synapses in the LNTB are large, and projections from globular bushy cells terminate upon the cell bodies of neurons in the LNTB (Smith *at al.*, 1991). Therefore the discharge patterns of these LNTB neurons, given a single super-threshold Hi-Sync input or several subthreshold Hi-Sync inputs, are also likely to be Hi-Sync.

The messages that one can take from our simulations are fairly straightforward. In order to attain realistic sensitivity to ITDs in response to tones, the model MSO cell requires the coincidence detecting mechanism and high synchronization to the stimulus in its inputs from the cochlear nucleus. The model presented here simulates physiological mechanisms that produce both coincidence detection in bushy cells and MSO cells and the generation of high-synchronization inputs to the MSO. In simulating excitatory and inhibitory responses to tones and clicks in the IC, we found that steady-state inhibitory activity must be weak in comparison with excitatory activity in order to maintain physiologically observed tone responses, and that large amounts of onset-driven inhibition were necessary to simulate responses to clicks similar to those observed in the IC. These simulation results point to the desirability of obtaining physiological responses to click stimuli in the MSO in order to evaluate the role of inhibition in the MSO.

Our results concerning the effect of onset driven inhibition on click responses apply more generally to the MSO/IC pathway than specifically to the MSO or IC, partly because we do not know the click response of an MSO cell. When click responses are recorded from MSO cells or their axons, the tone responses of these cells will be of interest to allow comparisons between transient and steady-state responses for individual neurons. If the click response to an MSO cell were to show strong evidence of onset-driven inhibition, the results of the simulations in this study would apply directly to the MSO cell. If not, it would then be of interest to determine where onset-driven inhibitory inputs that may affect the IC are generated, and how they act to shape the click responses observed in the IC.

Conclusions

- A computer model with physiologically reasonable assumptions provided an excellent description of MSO responses to tonal stimuli. Because this result can be obtained with or without inhibitory inputs, it appears that tonal stimuli are not appropriate for probing the role of inhibitory inputs to the MSO.
- Hi-Sync excitatory inputs are important for providing ITD sensitivity in discharge rate and synchronization index similar to that seen for tone responses in the MSO.
- Inhibitory inputs relayed from Hi-Sync globular bushy cells via inhibitory interneurons in the MNTB and LNTB cannot provide strong enough inhibition to MSO cells to be consistent with click responses in the IC without suppressing the sustained tone response below the levels observed in the MSO and IC.
- Onset and Pri-notch cells may provide patterns of inhibition to the MSO/IC pathway to reproduce observed IC click responses without suppressing the sustained tone responses observed in both the MSO and IC. In a model MSO cell with level-independent Onset inhibition, the dependence of click responses on stimulus intensity was similar to that observed in IC neurons.

ACKNOWLEDGMENTS

This work was supported by NIH Grant R01-DC00100 (HSC), and NIH Grant R29-DC01641 (LHC) from the National Institute of Deafness and other Communication Disorders, NIH.

REFERENCES

Adams, J. C. and Mugnaini, E. (1990). Immunocytochemical evidence for inhibitory and disinhibitory circuits in the superior olive. *Hearing Research 49*, 281–298.

Cant, N. B. and Hyson, R. L. (1992). Projections from the lateral nucleus of the trapezoid body to the medial superior olivary nucleus in the gerbil. *Hearing Research 58*, 26–34.

Carney, L. H. (1992). Modelling the sensitivity of cells in the anteroventral cochlear nucleus to spatiotemporal discharge patterns. *Phil. Trans. R. Soc. Lond. B 336*, 403–406.

Carney, L. H. (1993). A model for the response of low-frequency auditory-nerve fibers in cat. *J. Acoust. Soc. Am. 93(1)*, 401–417.

Carney, L. H. and Yin, T. C. T. (1989). Response of low-frequency cells in the inferior colliculus to interaural time differences of clicks: excitatory and inhibitory components. *J. Neurophysiol. 62(1),* 144–161.

Colburn, H. S., Han, Y. and Culotta, C. P. (1990). Coincidence model of MSO responses. *Hearing Research 49,* 335–346.

Durlach, N. I. and Colburn, H. S. (1978). Binaural Phenomena. In: *Handbook of Perception,* Vol. IV, Carterette, E. and Friedmann, M., eds. Academic Press, New York, chapter 10.

Eccles, J. C. *The Physiology of Synapses.* Academic Press, New York, 1964.

Frankhauser, B. and Moore, L. E. (1963). The effects of temperature on the sodium and potassium permeability changes in myelinated nerve fibers of *Xenopus laevis. J. Physiol. 169,* 431–437.

Gardner, M. B. (1968). Historical background of the Haas and/or precedence effect. *J. Acoust Soc. Am. 43,* 1243–1248.

Goldberg, J. M. and Brown, P. B. (1968). Functional organization of the dog superior olivary complex: an anatomical and electrophysiological study. *J. Neurophysiol. 31,* 639–656.

Goldberg, J. M. and Brown, P. B. (1969). Response of binaural neurons of dog superior olivary complex to dichotic tonal stimuli: some physiological mechanisms for sound localization. *J. Neurophysiol. 32,* 613–636.

Grothe, B. and Sanes, D. H. (1993). Bilateral inhibition by glycinergic afferents in the medial superior olive. *J. Neurophysiol. 69(4),* 1192–1196.

Han, Y. and Colburn, H. S. (1993). Point-neuron model for binaural interaction in MSO. *Hearing Research 68,* 115–130.

Haas, H. (1951). Uber den Einfluss eines Einfachechoes auf die Horsamkeit von Sprache. *Acustica* 1:49–58. English translation in: Haas, H. (1972). The influence of a single echo on the audibility of speech. *J. Audio Eng. Soc. 20,* 146–159.

Held, H. (1893). Die central Gehörleitung. *Archiv. Anat. Entwicklungsgesch 1g,* 201–248.

Hodgkin, A. L. and Huxley, A. F. (1952). A quantitative description of membrane current and application to conduction and excitation in nerve. *J. Physiol. 117,* 500–544.

Irvine, D. R. F. (1986). The auditory brainstem: a review of structure and function of auditory brainstem processing mechanisms. In: *Progress in Sensory Physiology,* Ottoson, D., ed. Springer-Verlag, Berlin, pp. 1–279.

Johnson, D. H. (1980). The relationship between spike rate and synchrony in responses of auditory-nerve fibers to single tones. *J. Acoust. Soc. Am. 68,* 1115–1122.

Joris, P. X., Carney, L. H., Smith, P. H. and Yin, T. C. T. (1994). Enhancement of synchronization in anteroventral cochlear nucleus. I. Responses to tones at characteristic frequency. *J. Neurophysiol. 71(3),* 1022–1036.

Liberman, M. C. (1991). Central projections of auditory-nerve fibers of differing spontaneous rates. *J. Comp. Neurol. 313,* 240–258.

Licklider, J. C. R. (1948). The influence of interaural phase relation on masking of speech by white noise. *J. Acoust. Soc. Am. 20,* 150–159.

Mardia, K. V. (1972). *Statistics of Directional Data,* Birnbaum, Z. W. and Lukacs, E., eds. Academic Press, New York.

Manis, P. B. and Marx, S. O. (1991). Outward currents in isolated ventral cochlear nucleus neurons. *J. Neurosci. 11(9),* 2865–2880.

Press, W. H., Flannery, B. P., Teukolsky, S. A. and Vetterling, W. T. (1986). *Numerical Recipes,* Press Syndicate of the Univ. of Cambridge, Cambridge, pp. 547–560.

Ramon y Cajal, S. (1909). *Histologie du systeme nerveux de l'homme et des vertebres.* Marloine, Paris.

Rayleigh, Lord. (1919). On the problem of random vibrations, and of random flights in one, two, or three dimensions. *Phil. Mag. 10,* 73–78.

Rose, J. E., Gross, N. B., Geisler, C. D. and Hind, J. E. (1965). Some neural mechanisms in the inferior colliculus of the cat which may be relevant to the localization of sounds. *J. Neurophysiol. 29,* 288–314.

Rothman, S. R., Young, E. D. and Manis, P. B. (1993). Convergence of auditory nerve fibers onto bushy cells in the ventral cochlear nucleus: implications of a computational model. *J. Neurophysiol. 70(6),* 2562–2583.

Rupert, A., Moushegian, G. and Whitcomb, M. A. (1966). Superior-olivary response patterns to monaural and binaural clicks. *J. Acoust. Soc. Am. 36,* 196–202.

Smith, P. H. (1995). Structural and functional differences distinguish principal from nonprincipal cells in the guinea pig MSO slice. *J. Neurophysiol. 73(4),* 1653–1667.

Smith, P. H., Joris, P. X. and Carney, L. H. (1991). Projections of physiologically characterized globular bushy cell axons from the cochlear nucleus of cat. *J. Comp. Neurol. 304,* 387–401.

Smith, P. H., Joris, P. X. and Yin, T. C. T. (1993). Projections of physiologically characterized spherical bushy cells axons from the cochlear nucleus of the cat: evidence for delay lines to the medial superior olive. *J. Comp. Neurol. 331,* 245–260.

Stutman, E. R. (1993). *A model for temporal sensitivity of neurons in the auditory brainstem: the role of a slow low-threshold potassium conductance.* Master's Thesis. Boston U., Boston, MA.

Yin, T. C. T. (1994). Physiological correlates of the precedence effect and summing localization in the inferior colliculus of the cat. *J. Neuroscience 14(9),* 5170–5186.

Yin, T. C. T., Chan, J. C. K. and Carney, L. H. (1987). Effect of interaural time delays of noise stimuli on low-frequency cells in the cat's inferior colliculus. III. Evidence for cross-correlation. *J. Neurophysiol. 58,* 562–583.

Yin, T. C. T. and Chan, J. C. K. (1990). Interaural time sensitivity in medial superior olive of cat. *J. Neurophysiol. 64(2),* 465–488.

Yin, T. C. T. and Kuwada, S. (1983). Binaural interaction in low frequency neurons in the inferior colliculus of the cat. III. Effects of changing frequency. *J. Neurophysiol. 50,* 1020–1042.

Yin, T. C. T. and Litovsky, R. Y. (1993). Physiological correlates of the precedence effect: Implications for neural models. *J. Acoust. Soc. Am. 93,* 2293.

Zurek, P. M. (1987). The precedence effect. In: *Directional Hearing,* Yost, W. A. and Gourevitch, G. eds., Springer-Verlag, New York, pp. 85–105.